arXiv:hep-th/0611157v2 28 Nov 2006

Self–accelerating Warped Braneworlds

Marcela Carena,[1] Joseph Lykken,[1] Minjoon Park,[2] and José Santiago[1]

[1] *Fermi National Accelerator Laboratory, P.O. Box 500, Batavia, IL 60510, USA*
[2] *Department of Physics, University of California, Davis, CA 95616, USA*

(Dated: February 2, 2008)

Braneworld models with induced gravity have the potential to replace dark energy as the explanation for the current accelerating expansion of the Universe. The original model of Dvali, Gabadadze and Porrati (DGP) demonstrated the existence of a "self–accelerating" branch of background solutions, but suffered from the presence of ghosts. We present a new large class of braneworld models which generalize the DGP model. Our models have negative curvature in the bulk, allow a second brane, and have general brane tensions and localized curvature terms. We exhibit three different kinds of ghosts, associated to the graviton zero mode, the radion, and the longitudinal components of massive graviton modes. The latter two species occur in the DGP model, for negative and positive brane tension respectively. In our models, we find that the two kinds of DGP ghosts are tightly correlated with each other, but are not always linked to the feature of self–acceleration. Our models are a promising laboratory for understanding the origins and physical meaning of braneworld ghosts, and perhaps for eliminating them altogether.

PACS numbers: 11.25.-w,04.50.+h,98.80.-k

I. INTRODUCTION

Models with extra spatial dimensions provide new perspectives on many long standing problems of particle physics and gravity. One of the most exciting suggestions [1, 2] is that an extra dimension, rather than dark energy, may be the origin of the currently accelerating expansion of the Universe. The original simple model of Dvali, Gabadadze and Porrati (DGP) posits that we live on a codimension one brane in an infinite flat five-dimensional bulk [3]. As generalized in [4], the model has only two relevant input parameters: a crossover scale r_c determined by the ratio of the 4d brane-localized gravity coupling with the 5d bulk one, and the tension of the brane. The Einstein equations have two kinds of solutions: a normal branch and a "self–accelerating" branch; both branches cause a modification of the effective 4d Friedmann equation, with the second one having the property that at sufficiently late times it gives an accelerated expansion without the need of dark energy to drive it.

The DGP model has encountered many difficulties, but the one that looks most serious is the presence of ghosts in the weakly–coupled long distance regime of the theory linearized around the self–accelerating background solution [4]-[6]. The physical origin and meaning of these ghosts are not yet clear.

Ghosts, like tachyons, are often an indication of an instability of the theory perturbed around a given background. Indeed it is not surprising that gravitating systems with nontrivial backgrounds including branes (in the absence of supersymmetry) exhibit a variety of instabilities. In the case of DGP, it is natural to ask whether modified brane setups might avoid ghosts and tachyons, while still exhibiting the key feature of self–acceleration.

In this paper we present a large class of warped brane setups that generalize the DGP model. Our basic idea is to use an AdS_5 bulk space, taking advantage of the fact that slices of AdS_5 can be flat, AdS_4, or dS_4. We consider models with one or two branes, taking the brane tensions and the brane-localized gravity couplings as input parameters, along with the bulk cosmological constant. We obtain background solutions with both normal and self–accelerating branches, for branes that are either AdS_4 or dS_4. The self–accelerating branches for the de Sitter branes give models precisely analogous to the DGP model; the self–accelerating branches for AdS_4 branes are not of obvious cosmological interest, but allow us to generalize the well-understood physics of the Karch-Randall model [7].

In two previous papers [8, 9] we set up the necessary tools to study generic warped models with arbitrary brane tensions and localized curvature terms. The size of the extra dimension and the brane curvature are well defined functions of the input brane parameters, and therefore by varying the latter we can parametrize a large number of different models. In one limit we make explicit contact with the original DGP model, while in another limit we reproduce the AdS_5/AdS_4 Karch-Randall model. In [8, 9] we studied the phenomenology of AdS_4 branes for background solutions on the standard branch, exhibiting a variety of ghosts and tachyons in parts of the parameter space of models. In this article we will extend that study to the self–accelerating branch and also consider the case in which the branes are dS_4. We will pay particular attention to the presence of ghosts in the spectrum and how this is related to which branch we are considering.

The outline of the paper is the following. In Section II we describe some basic facts about ghosts in theories with gravity. In Section III we review the main features of our new models, extending the results of [8, 9] to the self–accelerating branch and dS_4 branes. The spectrum, with particular emphasis on the presence of ghosts and tachyons,

is studied for the different cases in Section IV. Section V is devoted to our conclusions, and some technical details are relegated to appendices.

II. GHOSTS AND GRAVITY

With the (–+++) metric signature, a canonical scalar field kinetic action in flat space is written

$$\int d^4x \left(-\frac{1}{2}\eta^{\mu\nu}\partial_\mu\phi\partial_\nu\phi - \frac{1}{2}m^2\phi^2\right) . \tag{1}$$

Reversing the sign of the first term produces a ghost:

$$\int d^4x \left(\frac{1}{2}\eta^{\mu\nu}\partial_\mu\phi\partial_\nu\phi - \frac{1}{2}m^2\phi^2\right) . \tag{2}$$

As discussed *e.g.* in [10], defining the ghost propagator with the usual Feynman $i\epsilon$ prescription results in a nonunitary theory with negative norm states; defining the propagator with the opposite $i\epsilon$ prescription preserves unitarity but induces a catastrophic instability from propagating negative energy states.

Thus kinetic ghosts are similar to tachyons, in that they can be regarded as instabilities. Indeed some ghosts are also tachyons: this is the case in (2) for $m^2 > 0$, since the solutions of the wave equation will be exponentials rather than plane waves. As with tachyons, in some cases it may be possible to cure a ghost instability by perturbing around a different ground state. Such a shift can be thought of as the nonperturbative formation of a tachyon or ghost condensate; a tachyon condensate may produce a stable static ground state while a ghost condensate may produce a time dependent but ghost–free ground state [11].

In addition to ghosts and tachyons, one might worry that simple scalar field theories can suffer from other diseases. Suppose we add a derivative self-interaction term to (2):

$$\int d^4x \left(-\frac{1}{2}\eta^{\mu\nu}\partial_\mu\phi\partial_\nu\phi - \frac{1}{2}m^2\phi^2 + \frac{c}{2\Lambda^4}(\eta^{\mu\nu}\partial_\mu\phi\partial_\nu\phi)^2\right) , \tag{3}$$

where Λ is the UV cutoff of this effective theory. For $c < 0$, this theory appears to have analyticity problems and exhibits superluminal modes in the massless limit, despite a lack of tachyonic instability [12]. However Jenkins and O'Connell have recently shown [13] that "positivity constraints" of this type are equivalent to a no–tachyon condition in a (partial) UV completion. In other words, effective theories of the form (3) with $c < 0$ arise from integrating out tachyons before curing the tachyonic instability. Thus kinetic ghost and tachyon instabilities appear to exhaust the physically distinct diseases of scalar field theories.

This simple picture, however, is intrinsic to flat space propagators and flat space kinetic terms. Adding gravity to the picture complicates the discussion of ghosts, and has led to much debate in the literature. Once we add gravity, we must be on the lookout for new kinds of ghosts. In addition to scalar ghosts, the longitudinal mode of a massive graviton can be a ghost. As we will see, even a massless graviton can be a ghost. Because gravity is a nonlinear theory with a large local symmetry, we must also work harder to understand the physical significance of ghosts.

A. de Sitter ghosts

It was shown many years ago by Higuchi [14] that the longitudinal modes of massive gravitons can be ghosts if we are in a de Sitter background. Letting $12\mathcal{H}^2$ denote the constant de Sitter curvature, massive gravitons with mass in the range $0 < m^2 < 2\mathcal{H}^2$ are ghosts. These correspond to nonunitary representations of the de Sitter group $SO(4,1)$, as discussed in [15, 16], but the analysis of Deser and Waldron [17] shows that they are also kinetic ghosts. As we will see in the next section using an explicit on-shell tensor decomposition, the effective kinetic term of a longitudinal massive graviton mode $s(x)$ in a dS_4 background is given by:

$$\frac{3}{2}m^2(m^2 - 2\mathcal{H}^2)\int d^4x\, s(x)\left(-\partial_0^2 + \nabla_i^2 - (m^2 - \frac{9}{4}\mathcal{H}^2)\right)s(x) , \tag{4}$$

where ∇_i^2 is the de Sitter Laplacian $\nabla_i^2 = \partial_i^2/f(t)^2$, with $f(t) = \exp(\mathcal{H}t)$ coming from the dS_4 background metric: $g_{00} = -1$, $g_{ij} = f^2\delta_{ij}$. From (4) we see immediately that the longitudinal mode is a ghost for $0 < m^2 < 2\mathcal{H}^2$. It would also naively appear that the longitudinal mode is a tachyon for $0 < m^2 < \frac{9}{4}\mathcal{H}^2$. However the analysis of tachyonic

instabilities in dS_4 is complicated by the fact that the naive Hamiltonian corresponding to the wave operator in (4) has an explicit time-dependence from $f(t)$ and is therefore not conserved. The operator corresponding to the actual conserved energy is manifestly positive *inside the de Sitter horizon* for any $m^2 > 0$, as shown in [17]. This is referred to as a "mild" tachyonic instability in the last reference in [4]; for our purposes we will not call such modes tachyons, reserving that name for cases such as $m^2 < 0$ in (4) which resemble tachyons in flat space.

It was shown in [4] that the DGP model with positive brane tension contains a longitudinal massive graviton mode ghost on the self–accelerating branch. Intriguingly, for negative brane tension the massive graviton ghost is absent, replaced instead by a ghost radion scalar. In the warped models presented in the paper, we will find that these two kinds of ghosts are also tightly related.

The physical interpretation of ghosts in theories with gravity can be obscured by the presence of local symmetries. For example the DGP model in the limit of a tensionless brane has a massive graviton mode with $m^2 = 2H^2$; the resulting 4d massive gravity theory has an enhanced "accidental" local symmetry beyond 4d general covariance [18, 19]. Charmousis *et al.* found a ghost in this limit as well [4], but Deffayet *et al* have argued [20] that this mode is actually a Lagrange multiplier enforcing an explicit gauge-fixing of the extra symmetry. This is an interesting special case to be considered elsewhere.

B. when a ghost is not a ghost

It can be argued (incorrectly) that gravity renders the physical meaning of ghosts ambiguous. Consider, for example, pure 4d Einstein gravity. Perform a conformal rescaling of the metric by the field redefinition

$$g_{\mu\nu} \to \left(1 + \frac{\phi}{M}\right) g_{\mu\nu} \ , \tag{5}$$

where $\phi(x)$ is a 4d scalar field and M is the reduced Planck mass. Now substitute the rescaled metric into the Einstein-Hilbert action, assuming that the background metric before rescaling was flat:

$$\sqrt{-g}\, M^2 R \to \frac{3}{2}\, \frac{1}{1+\phi/M}\, \eta^{\mu\nu} \partial_\mu \phi \partial_\nu \phi \ . \tag{6}$$

This looks like a kinetic ghost. Now suppose we start with a Lagrangian whose perturbation theory around flat space is obviously ghost-free:

$$\int d^4x \sqrt{-g} \left(M^2 R - \frac{1}{2}\, g^{\mu\nu} \partial_\mu \phi \partial_\nu \phi \right) \ . \tag{7}$$

It appears naively that by a simple field redefinition of the metric we can produce a ghost.

The flaw in this argument is that we have ignored the subtleties of general covariance and gauge-fixing [20]. Consider again 4d Einstein gravity expanded around flat space: $g_{\mu\nu} = \eta_{\mu\nu} + h_{\mu\nu}$. As discussed in [8], the massless symmetric tensor $h_{\mu\nu}$ can be decomposed as

$$h_{\mu\nu} = \beta_{\mu\nu} + \partial_\mu v_\nu + \partial_\nu v_\mu + \partial_\mu \partial_\nu \varphi_1 + c_{\mu\nu} + \partial_\mu n_\nu + \partial_\nu n_\mu + \eta_{\mu\nu} \varphi_2 \ . \tag{8}$$

Here $\beta_{\mu\nu}$ is traceless, transverse, and orthogonal to n_μ, giving 2 degrees of freedom. Similarly v_μ is transverse and orthogonal to n_μ, giving 2 degrees of freedom, while the longitudinal null vector n_μ gives 1 more degree of freedom. Lastly, $c_{\mu\nu}$ is traceless but not transverse, giving 3 degrees of freedom, which together with the two scalars φ_1 and φ_2 adds up to the total 10 degrees of freedom of $h_{\mu\nu}$.

Obviously v_μ, n_μ and φ_1 are the 4 pure gauge modes of 4d general covariance, while $\beta_{\mu\nu}$ gives the two traceless transverse propagating degrees of freedom of an on-shell massless graviton. The four remaining degrees of freedom represented by φ_2 and $c_{\mu\nu}$ are subject to constraints from the equations of motion. In the absence of sources they are constrained to vanish. Just as for the more familiar case of the time-like component of an abelian gauge field, these modes do not really propagate. In the post-Newtonian approximation [21], φ_2 is proportional to the Newtonian scalar potential (analogous to the electrostatic potential) while $c_{\mu\nu}$ contains the Newtonian vector potential. So φ_2 represents the same kind of ghost as the time-like component of an abelian gauge field (which in the nonrelativistic limit gives the electrostatic potential). Such ghosts are not really ghosts since they do not propagate: the corresponding degrees of freedom are completely fixed in terms of sources by solving constraints from the equations of motion.

Thus the metric rescaling (5) in the theory described by (7) mixes a non-ghost matter scalar with a pseudo-ghost mode of the metric. The full quadratic action of the rescaled theory will have kinetic terms mixing ϕ with φ_2. Presented with such an action *ab initio*, the proper way to extract its physical degrees of freedom is to gauge–fix it and diagonalize the kinetic terms. The only way to diagonalize the kinetic terms is by shifting $\varphi_2 \to \varphi_2 - \phi/M$, effectively undoing the metric rescaling (5). The theory is then obviously free of ghosts.

C. summary

The moral of this story is that there is an unambiguous procedure for determining the presence of ghosts in a theory with gravity expanded around a given background solution. First, determine the local symmetries and gauge–fix them. Second, diagonalize the full quadratic action. Third, extract the propagators of the physical degrees of freedom and check for kinetic ghosts. It is also important to check for tachyons; in our dS_4 example above, the longitudinal graviton mode $s(x)$ for $m^2 < 0$ is an example of a tachyon which is not a ghost.

As we argued above, for scalars in flat space ghosts and tachyons exhaust the list of physically distinct pathologies for weakly coupled theories. This is less obvious for gravity. However if we avoid regions of strong coupling and abstain from integrating out degrees of freedom, there does not seem to be any reason to impose additional positivity constraints. We will assume this for our analysis.

There is one other possible source of ambiguity. Because gravity is a highly nonlinear theory, one could imagine that there are physical setups in which even the long–range solutions are intrinsically nonlinear. In such a case ghosts of the linearized solutions are irrelevant, since the linearized solution is not itself an approximation to the real solution, even very far away from any source. It has been argued that this may occur in the DGP model [22]. Note that the claim that nonlinearities of gravity are important at cosmological scales is different from the claim that matter nonlinearities are important at cosmological scales [23]; the latter has also been suggested as a replacement for dark energy in explaining late time accelerated expansion [24]. At any rate we will not pursue this idea here, since we find the linearized analysis of our models quite challenging enough!

III. WARPED MODELS WITH INDUCED GRAVITY

In this section we will review the main features of the two-brane models introduced in [8, 9], extending the results to include the self–accelerating branch and the case of positively curved dS_4 branes. The model is described by the following action

$$\begin{aligned} S \;=\; & \int d^4x \int_{0^+}^{L^-} dy\sqrt{-G}\Big(4M^3R - 2\Lambda\Big) \\ & + \sum_i \int_{y=y_i} d^4x\sqrt{-g^{(i)}}(2M_i^2\tilde{\mathcal{R}}^{(i)} - V_i) + 4M^3\oint_{\partial\mathcal{M}} K\,. \end{aligned} \tag{9}$$

This action represents a general warped gravity setup with codimension one branes, written in the interval picture. We have only displayed one interval since physics on the second interval is fixed by a $\mathbf{Z_2}$ symmetry. In (9) M is the 5d Planck scale, $\Lambda = -24M^3k^2$ is the bulk cosmological constant giving a bulk curvature k, the M_i are the coefficients of brane-localized curvatures $\tilde{\mathcal{R}}^{(i)}$, the V_i are brane tensions and K is the trace of extrinsic curvature. As described in [8] we will use the straight gauge formalism to keep the brane locations fixed at $y = 0^+$ and $y = L^-$, even in the presence of linearized fluctuations of the metric. There are no "brane-bending" modes in a straight gauge.

The background solution can be written as

$$ds^2 = G_{MN}dx^M dx^N = g_{\mu\nu}dx^\mu dx^\nu + dy^2, \tag{10}$$

where y is restricted to the interval $0 < y < L$ and

$$g_{\mu\nu} = a^2(y)\gamma_{\mu\nu}\,, \tag{11}$$

with $\gamma_{\mu\nu}$ the metric of dS_4 or AdS_4 with constant curvature $12\mathcal{H}^2$. The explicit form of the warp factor, $a(y)$, the 4d curvature constant $\mathcal{H}^2$, and the coordinate size of the extra dimension L, depend on the input brane parameters that also determine how the AdS_5 bulk is sliced. It is convenient to define the brane parameters in terms of dimensionless quantities,

$$v_i = kM_i^2/M^3, \quad w_i = V_i/2kM^3\,. \tag{12}$$

The derived features of the model are determined by the following combinations of input parameters:

$$T_i^\pm \equiv \frac{1}{v_i}\left(-1 \pm \sqrt{1 + v_iw_i/6 + v_i^2}\right)\,. \tag{13}$$

The choice of sign in (13) corresponds to the two independent branches (per brane) of the background solutions to the equations of motion.

A. slicing the $\mathbf{AdS_5}$ bulk

For a given set of five input parameters k, v_0, w_0, v_L, w_L, the first question is to determine the possible dS_4 or AdS_4 slicings of the AdS_5 bulk. This is set by whether the absolute value of T_i is larger or smaller than one. We show in Figure 1 the regions in the (v, w) plane that correspond to $|T| > 1$ with dark shade and $|T| < 1$ in light shade. In the unshaded regions T is complex. The left and right panels are for T^+ and T^-, respectively. The curved boundaries correspond to the line $w = -6(1 + v^2)/v$, the horizontal lines that separate the dark and light areas correspond to $w = \pm 12$ (and v smaller or larger than ± 1, depending on the panel) and finally the slanted line on the left panel separating the two light shades (with T^+ positive or negative) corresponds to $w = -6v$.

Simply put, in the dark shaded regions the branes are both dS_4, in the light shaded regions they are both AdS_4. We parametrize the warp factor differently in each case:

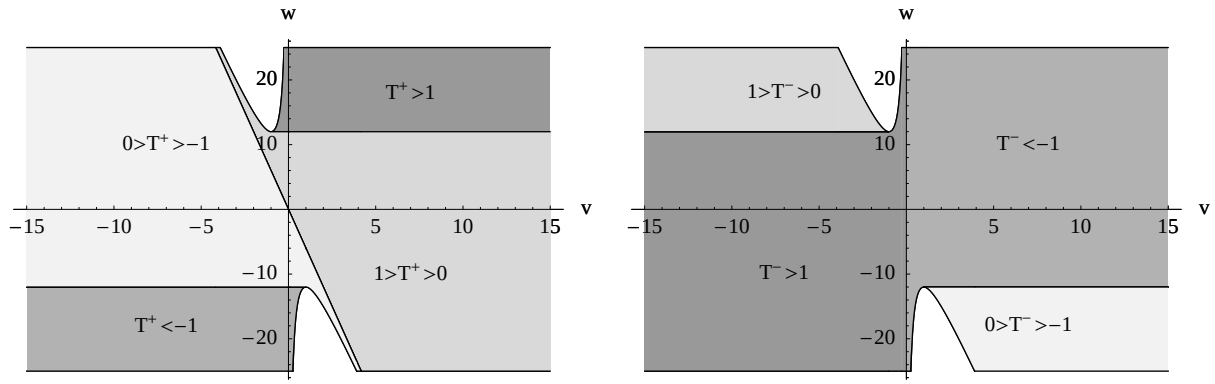

FIG. 1: Regions of the (v, w) plane corresponding to different background solutions and signs of T. The left panel is for the T^+ branch and the right panel is for the T^- branch. The two (lighter) darker shades correspond to $(A)dS_4$ branes. In the unshaded regions the branes are neither AdS_4 nor dS_4.

- **$\mathbf{AdS_5}$/$\mathbf{AdS_4}$**: If $|T_i| < 1$, then the branes are AdS_4. The warp factor reads,

$$a(y) = \frac{\cosh k(y - y_0)}{\cosh k y_0}, \tag{14}$$

with the turning point y_0 and L given by

$$T_0 = \tanh k y_0, \quad T_L = \tanh k(L - y_0). \tag{15}$$

Note that the requirement $L > 0$ implies

$$T_0 + T_L > 0. \tag{16}$$

Finally the brane curvature is given by ($\mathcal{H}^2 \equiv -H^2 < 0$)

$$H = \frac{k}{\cosh k y_0}. \tag{17}$$

- **$\mathbf{AdS_5}$/$\mathbf{dS_4}$**: If $|T_i| > 1$, then the branes are dS_4. The warp factor reads,

$$a(y) = -\frac{\sinh k(y - y_0)}{\sinh k y_0}, \tag{18}$$

with y_0 and L given by

$$T_0 = \coth k y_0, \quad T_L = \coth k(L - y_0). \tag{19}$$

Note that if $0 < y_0 < L$, the warp factor vanishes at some point in the bulk. This is a true singularity and therefore does not give rise to an acceptable model. Thus we have to require either $y_0 < 0$ or $y_0 > L$ for the case of dS_4 branes. This requirement, together with $L > 0$, implies the conditions

$$T_0 \cdot T_L < 0, \quad T_0 + T_L < 0. \tag{20}$$

Finally the brane curvature is given by

$$\mathcal{H} = \tilde{\epsilon}_0 \frac{k}{\sinh k y_0}, \tag{21}$$

where $\tilde{\epsilon}_0$ is the sign of T_0.

B. standard branches and self–accelerating branches

For fixed input brane parameters, we have two different background solutions per brane, denoted by the sign choice $\epsilon_i = \pm$ in $T_i^{\epsilon_i}$ (not to be confused with $\tilde{\epsilon}_i$, the sign of T_i itself). These two branches exhibit different physical features. In the following, we will focus our attention to the brane at $y = 0$. The restriction $L > 0$, in addition to $y_0 < 0$ or $L < y_0$ for dS_4 branes, will then imply restrictions on the parameters of the brane located at $y = L$, such that not all combinations of signs give sensible solutions.

The choice of branch for the brane at $y = 0$, *i.e.* the choice of ϵ_0, corresponds to the standard and self–accelerating branches for the cosmology of brane–induced gravity. In our notation, the standard branch corresponds to T_0^+ whereas the T_0^- branch is the self–accelerating one. The reason is the following. For fixed values of the brane parameters, v_0, w_0, the brane curvature is larger for the self–accelerating branch than for the standard one[1]. This is obvious for $|w_0| < 12$, for which T_0^+ corresponds to AdS_4 solutions whereas T_0^- gives a dS_4 brane (see Fig. 1). In the rest of the parameter space, where we have either two AdS_4 or two dS_4 solutions, it is still true that

$$\mathcal{H}^2\left[T_0^+(v_0, w_0)\right] < \mathcal{H}^2\left[T_0^-(v_0, w_0)\right]. \tag{22}$$

Furthermore, for positive v_0, the Randall-Sundrum [26] tuning $w_0 = +12$ results in a flat brane (independently of the particular value of v_0) for T_0^+ and an inflating brane for T_0^-, thus the names standard and self–accelerating branches. This is the exact warped analogue of the DGP tensionless brane. In the following we will loosely use the term branch to denote the choice of sign in either brane. However, as we said, it is the brane at $y = 0$ that determines the standard or self–accelerating nature of the solution, and therefore we will only apply these terms to the brane at $y = 0$.

C. properties of the spectrum

The properties of the physical spectrum were described for the AdS_4 brane case in [8, 9], and can be easily extended to the dS_4 case. The spectrum is obtained by computing the action at the quadratic level for small perturbations around the background metric,

$$G_{MN} \to G_{MN} + h_{MN}. \tag{23}$$

This can be done in a straight gauge, for which the branes are straight and at fixed positions, $y = 0^+, L^-$, and $h_{\mu 4}(x, y) = 0$. A further gauge–fixing exhibits the radion,

$$h_{44}(x, y) = F(y)\psi(x), \tag{24}$$

where $F(y)$ is a fixed but arbitrary function (part of the gauge choice) and $\psi(x)$ is a four-dimensional scalar. The components of $h_{\mu\nu}(x, y)$ can then be shown to have the following 4d physical degrees of freedom:

- **massless modes**: there is a graviton zero mode, $B_{\mu\nu}(x)$ (2 degrees of freedom) and the above mentioned radion, $\psi(x)$.

$$h_{\mu\nu} = a^2(y)B_{\mu\nu}(x) + a^2\mathcal{Y}_1(y)\tilde{\nabla}_\mu\tilde{\nabla}_\nu\psi + g_{\mu\nu}\mathcal{Y}_2(y)\psi\,. \tag{25}$$

  where the y dependence in the radion piece is given by

$$\mathcal{Y}_1(y) = \chi\frac{k}{\mathcal{H}^2}(z-1)^2 - \mathfrak{F}\,, \quad \mathcal{Y}_2(y) = \chi k(z-1)^2 + \frac{a'}{a}\mathcal{F}\,. \tag{26}$$

---

[1] The name self–accelerating is actually a bit of abuse of language in these more general configurations as there are regions of parameter space where the T_0^- branch gives an AdS_4 background, which is never accelerating. Nevertheless even in this case there is a net positive contribution to the brane curvature as compared with the standard branch.

In this last equation we have defined the variable z

$$z = \begin{cases} \tanh k(y-y_0), & \mathcal{H}^2 < 0, \\ \coth k(y-y_0), & \mathcal{H}^2 > 0. \end{cases} \tag{27}$$

Note that we have $T_i = \theta_i z(y_i)$, with $-\theta_0 = \theta_L = 1$. χ, $\mathcal{F}$ and $\mathfrak{F}$ are remnants of the residual gauge freedom (related to $F(y)$) whose detailed form is not important for the discussion below.

- **massive modes**: there is a tower of massive gravitons (5 degrees of freedom each)

$$h_{\mu\nu} = \sum_q b^{(q)}_{\mu\nu} = \sum_q \mathcal{Y}^{(q)}(y) B^{(q)}_{\mu\nu}(x)\,, \tag{28}$$

where q labels the mass, $q = m^2/\mathcal{H}^2$, and

$$\begin{aligned} \mathcal{Y}^{(q)}(y) &= P^{-2}_{(-1+\sqrt{9-4q})/2}(z) - \frac{a_0^{(q)}}{b_0^{(q)}} Q^2_{(-1+\sqrt{9-4q})/2}(z) \\ &= P^{-2}_{(-1+\sqrt{9-4q})/2}(z) - \frac{a_L^{(q)}}{b_L^{(q)}} Q^2_{(-1+\sqrt{9-4q})/2}(z)\,, \end{aligned} \tag{29}$$

where the P's and Q's are associated Legendre functions. The mass spectrum of modes is determined by solving the determinant equation,

$$a_0 b_L - a_L b_0 = 0\,, \tag{30}$$

with

$$a_i = 2\theta_i(1-T_i^2)\frac{d}{dz}P^{-2}_{-\frac{1}{2}+\frac{1}{2}\sqrt{9-4q}}(z)\Big|_{z=\theta_i T_i} - \{v_i q(T_i^2-1)+4T_i\}P^{-2}_{-\frac{1}{2}+\frac{1}{2}\sqrt{9-4q}}(\theta_i T_i)\,, \tag{31}$$

$$b_i = 2\theta_i(1-T_i^2)\frac{d}{dz}Q^2_{-\frac{1}{2}+\frac{1}{2}\sqrt{9-4q}}(z)\Big|_{z=\theta_i T_i} - \{v_i q(T_i^2-1)+4T_i\}Q^2_{-\frac{1}{2}+\frac{1}{2}\sqrt{9-4q}}(\theta_i T_i)\,. \tag{32}$$

All these equations are valid for both signs of the brane curvature, provided the right definition of z, the warp factor, $a(y)$, and the sign of the brane curvature $\mathcal{H}^2$ are used.[2] Performing the integration over the extra dimension in the quadratic terms for the different modes we obtain the corresponding kinetic coefficients (normalization constants). For the massless modes:

$$\mathcal{C}_g^{(0)} = \frac{T_0^2-1}{k}\sum_i \left[-ky_i + \frac{T_i+v_i}{T_i^2-1}\right], \tag{33}$$

$$\mathcal{C}_\psi = -\frac{3\chi^2\mathcal{H}^2}{2k}\sum_i \left[T_i + \frac{v_i+T_i}{1+v_iT_i}\right], \tag{34}$$

and for the massive modes:

$$\mathcal{C}_g^{(q)} = -\frac{k}{\mathcal{H}^2}\Big(2\int_{-T_0}^{T_L}\mathcal{Y}^{(q)2}\mathrm{d}z + \sum_i [v_i(1-z^2)\mathcal{Y}^{(q)2}]_{z=\theta T_i}\Big)\,. \tag{35}$$

If any of these coefficients becomes infinite, the corresponding mode is not normalizable and decouples from the spectrum. If it vanishes, then we are in a region of strong coupling. If it becomes negative, then the mode is a ghost.

---

[2] The price for this convenient notation is that q as defined here is $-q$ as defined in [8].

D. longitudinal graviton modes in dS_4

As already mentioned, for dS_4 the kinetic terms of some massive graviton modes have an intrinsic mass-dependent kinetic coefficient already at the 4d level, in addition to the overall coefficient $\mathcal{C}_g^{(q)}$ that they inherit from the Kaluza-Klein (KK) decomposition. Thus in this case we need to compute this intrinsic coefficient before deciding if the mode is a ghost.

To compute these coefficients, we need an explicit orthogonal decomposition of the five "helicities" of each massive 4d graviton $B_{\mu\nu}^{(q)}(x)$. The appropriate orthogonal decomposition turns out to be:

$$\begin{aligned} B_{00}^{(q)}(x) &= f^{-3/2}\nabla_k^2 s^{(q)}(x) \,, \\ B_{0i}^{(q)}(x) &= f^{1/2}\nabla_k^2 v_i^{(q)}(x) + f^{-2}\partial_0\partial_i(f^{1/2}s^{(q)}(x)) \,, \\ B_{ij}^{(q)}(x) &= f^{1/2}b_{ij}^{(q)}(x) + f^{-1}\partial_0(f^{3/2}(\partial_i v_j^{(q)}(x) + \partial_j v_i^{(q)}(x))) \\ &\quad + \frac{1}{2}f^{1/2}P_{ij}\nabla_k^2 s^{(q)}(x) + (\delta_{ij} - \frac{3}{2}P_{ij})\partial_0(\partial_0 + H)(f^{1/2}s^{(q)}(x)) \,, \end{aligned} \tag{36}$$

where

$$P_{ij} \equiv \delta_{ij} - \frac{\partial_i\partial_j}{\partial_k^2} \tag{37}$$

is a transverse projection operator in the flat 3d sense, and $\nabla_i^2 = \partial_i^2/f(t)^2$ is the 3d Laplacian defined already in the previous section. In (36) the $b_{ij}^{(q)}(x)$ are traceless-transverse in the flat 3d sense (2 degrees of freedom), corresponding to the helicity ± 2 modes of the massive gravitons in the KK tower. The $v_i^{(q)}(x)$ are transverse vectors in the flat 3d sense (2 degrees of freedom), corresponding to the helicity ± 1 modes of the massive gravitons in the KK tower. The $s^{(q)}(x)$ are the longitudinal modes of the massive gravitons.

Substituting the ansatz (36), it is straightforward but tedious to show that the full 5d bulk equations of motion reduce to a set of constraint equations which are automatically satisfied, together with the following dynamical 4d equations of motion in the de Sitter background:

$$\begin{aligned} 0 &= \left(-\partial_0^2 + \nabla_i^2 - (m^2 - \frac{9}{4}\mathcal{H}^2)\right) b_{ij}^{(q)}(x) \,, \\ 0 &= \nabla_j^2 \left(-\partial_0^2 + \nabla_i^2 - (m^2 - \frac{9}{4}\mathcal{H}^2)\right) v_i^{(q)}(x) \,, \\ 0 &= \nabla_j^2 \left(-\partial_0^2 + \nabla_i^2 - (m^2 - \frac{9}{4}\mathcal{H}^2)\right) s^{(q)}(x) \,. \end{aligned} \tag{38}$$

Solutions to the equation of motion for the vectors $v_i^{(q)}(x)$ and scalars $s^{(q)}(x)$ appear to be defined only up to an arbitrary harmonic function annihilated by ∇_i^2, but a residual 4d general coordinate invariance removes this ambiguity.

We can also substitute our orthogonal decomposition (36) into the effective 4d quadratic action, to read off the intrinsic mass-dependent kinetic coefficients. Since the decomposition involves derivatives, this is really only meaningful with the derivatives evaluated on-shell. The interesting case is for the longitudinal modes, where after another tedious calculation we obtain the effective action shown in (4) for each longitudinal graviton mode in the KK tower. Thus, even for values of $q = m^2/\mathcal{H}^2$ such that $\mathcal{C}_g^{(q)} > 0$, the longitudinal graviton mode will be a ghost if $0 < q < 2$.

IV. GHOSTS IN MODELS WITH INDUCED GRAVITY

In this section we will discuss the spectrum of our models in the search of regions that are free of ghost and tachyonic instabilities. This is done by studying the solutions of the eigenvalue equation for the massive modes (30) as well as the kinetic coefficients of these and the graviton zero mode and radion, (33-35). It is useful to separate the discussion for AdS_4 and dS_4 branes, because of the different behavior of the longitudinal component of massive gravitons in the latter. Thus, in an AdS_4 space, we only need to look at the kinetic coefficients of the different modes, ghosts being uniquely determined by the negative sign of their kinetic terms, whereas in dS_4 space, the longitudinal component of a massive graviton with positive overall kinetic coefficient but with mass $0 < m^2 < 2H^2$ is a ghost, becoming a (non-ghost) tachyon for $m^2 < 0$.

A. negative curvature: AdS_4 branes

The presence of ghosts for AdS_4 branes was discussed, for the standard branch, in [9]. In this section we will review the results and generalize them to the self–accelerating branch. Let us start discussing the simpler case of the graviton zero mode. Recalling the definition of T_i in the AdS_4 background (15), we can write the kinetic coefficient for the graviton zero mode as

$$\mathcal{C}_g^{(0)AdS_4} = \frac{1-T_0^2}{k}\sum_i \left[\tanh^{-1} T_i + \frac{T_i+v_i}{1-T_i^2}\right]. \tag{39}$$

For AdS_4 the global term outside the sum is positive so we only need to look at the sign of the sum. Let us define each term in the sum as

$$\bar{\mathcal{C}}_g^{(0),i} \equiv \tanh^{-1} T_i + \frac{v_i+T_i}{1-T_i^2}. \tag{40}$$

$\bar{\mathcal{C}}_g^{(0),i}$ is a growing function of w_i, for fixed v_i. Let us now consider its value at the boundaries of the AdS_4 region in the (v,w) plane (light shaded areas in Fig. 1). In the limit $v_i \to \pm\infty$ along the curve $w_i = -6(1+v_i^2)/v_i$ we get $\mathcal{C}_g^{(0),i} = \pm\infty$. As we move along that curve towards the points $v_i \to \pm 1$ (and $w_i = \mp 12$, respectively), it goes to $\mp\infty$. This is independent of which branch we have chosen for the branes. The rest of the boundaries, however, depend on whether we have T_i^+ or T_i^- (see Fig. 1). For T_i^+, $\bar{\mathcal{C}}^{(0),i}$ stays $+\infty$ for $w_i = +12$ and $v_i > -1$ and $-\infty$ for $w_i = -12$ and $v_i < 1$ whereas for T_i^- it is $-\infty$ for $w_i = +12$, $v_i < -1$ and $+\infty$ for $w_i = -12$ and $v_i > 1$. In summary, for any branch it goes all the way to $-\infty$ for negative v_i and all the way to $+\infty$ for positive v_i. Furthermore it can be made as negative (positive) as one wants for sufficiently large negative (positive) v_i. Thus, it is clear that independent of the value of $\bar{\mathcal{C}}_g^{(0),L}$ (provided it remains finite) there will always be a curve splitting the (v_0, w_0) plane in two parts, such that to the left of the curve the graviton zero mode is a ghost and to the right of the curve it is not. The case of the radion is more complicated so rather than giving analytic expressions describing the different behaviors, we prefer to show, directly in the figures, the relevant cases for the different choices of branches.

There is also an extra source of instability in these models, namely the possible existence of tachyons in the spectrum. A thorough study of tachyons for the case of AdS_4 branes in the standard branch was done in [9], and the techniques to study them apply mostly unchanged to the self–accelerating branch. Recall that in our notation, due to $\mathcal{H}^2(AdS_4) < 0$, tachyonic solutions are characterized by $q > 0$. It proves useful to study the behavior of the quantity

$$\mathfrak{D} \equiv \frac{a_0 b_L - b_0 a_L}{q(1-T_0^2)(1-T_L^2)}, \tag{41}$$

that has the same massive solutions as our original eigenvalue equation, but we have explicitly removed the zero mode solution, $q = 0$. The behavior of this function at $q = 0$ and $q \to \infty$ is, respectively [9],

$$\mathfrak{D}(q=0) = 2\frac{k}{T_0^2-1}\mathcal{C}_g^{(0)}, \tag{42}$$

and

$$\text{sign}\big[\mathfrak{D}(q\to\infty)\big] = \text{sign}\big[v_0 v_L(\cos^{-1} T_0 + \cos^{-1} T_L - \pi)\big]. \tag{43}$$

Thus, if the signs of both are different, there exists an odd number (therefore at least one) of solutions with positive q, *i.e.* tachyons. If the signs of both are the same, then there is either no tachyon or an even number of them (that last distinction can be resolved numerically). The condition $L > 0$ gives, for AdS_4 branes, $T_0 + T_L > 0$ which in turn implies

$$\cos^{-1} T_0 + \cos^{-1} T_L - \pi < 0. \tag{44}$$

It is then clear that in order to have an even number of tachyons (usually zero), we need

$$\text{sign } v_0 v_L = \text{sign } \mathcal{C}_g^{(0)} > 0, \tag{45}$$

where the last inequality is for the phenomenologically relevant region in which the graviton zero mode is not a ghost.

In Fig. 2 we show the case of the (T_0^+, T_L^+) branch for two possible behaviors, depending on which choice of parameters we make for the brane at $y = L$. We represent three different shades in the figure, the light one is the

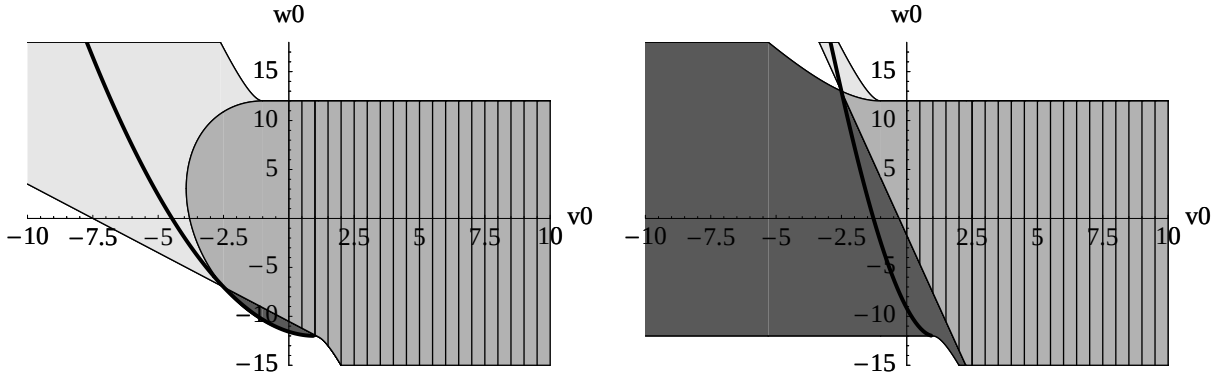

FIG. 2: Ghost and tachyon–free region for the (T_0^+, T_L^+) branch. The different shades correspond to the following regions: $L > 0$ (light), $\mathcal{C}_\psi > 0$ (dark) and the intersection of both (intermediate). The hatched area corresponds to the region where $\mathcal{C}_\psi > 0$, $L > 0$ and there are not tachyons in the spectrum. The region to the right of the thick solid line corresponds to $\mathcal{C}_g^{(0)} > 0$. Thus, the hatched area to the right of that line is the ghost and tachyon–free region for this configuration. In the left panel $v_L = 2.5$, $w_L = 7$ whereas in the right panel we use $v_L = 2.5$ and $w_L = -13$.

region of parameter space for which $L > 0$, the dark one is the region in which the radion is not a ghost and the intermediate shade is the region for which both conditions are satisfied. That latter area is hatched if no tachyons are present in the spectrum. In these examples we have $v_L = 2.5 > 0$ and therefore the condition for no tachyons in the spectrum demands $v_0 > 0$. Finally, the thick solid line represents the points for which $\mathcal{C}_g^{(0)} = 0$. Therefore the hatched region to the right of the solid line is ghost and tachyon free. (It can be checked numerically that the massive gravitons have positive kinetic coefficients in that region.) Note that there are also regions of parameter space with positive and small v_0 that are not allowed.

In Fig. 3, we consider the case of the (T_0^+, T_L^-) branch. In this case there is a large region where the radion is not a ghost for both values of the sign of v_0, provided $w_L > 12$ (considering values of $w_L < -12$ yields a very small region for which the radion is not a ghost). In the figure, we have chosen $v_L = -4$ and $w_L = 15$. The shades have the same

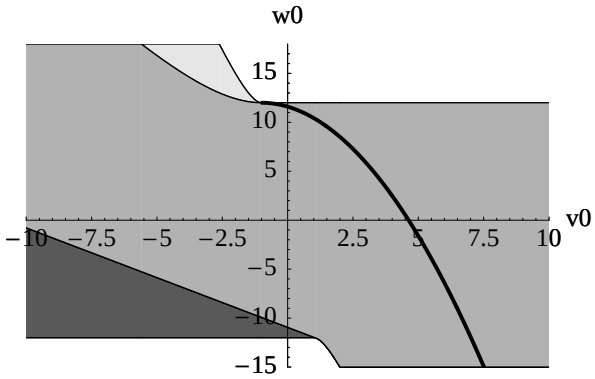

FIG. 3: Ghost-free region for the (T_0^+, T_L^-) branch, with $w_L > 12$. We have taken $v_L = -4$ and $w_L = 15$. The region to the right of the thick solid line corresponds to $\mathcal{C}_g^{(0)} > 0$. The shades correspond to the following regions: $L > 0$ (light), $\mathcal{C}_\psi > 0$ (dark) and the intersection of both (intermediate). The ghost–free region has tachyons in the spectrum.

meaning as in the previous figure. From Fig. 1, it follows that $w_L > 12$ implies $v_L < 0$ for T_L^-, thus the region to the right of the graviton zero mode line with $v_0 > 0$ has an odd number of tachyons. A numerical analysis shows that the small region to the right of the graviton zero mode line but with $v_0 < 0$ has two tachyons. Thus, this solution does not have any region that is ghost and tachyon free (no hatched area).

Let us consider now the cases of self–accelerating branches: (T_0^-, T_L^-) and (T_0^-, T_L^+). In Fig. 4 we show the case (T_0^-, T_L^-). There is a large ghost–free region in the case that $w_L > 12$ whereas it shrinks to almost nothing if $w_L < -12$. From Fig. 1, it follows that $w_L > 12$ implies $v_L < 0$ (left panel in the Fig. 4) and $w_L < -12$ implies $v_L > 0$ (right panel). The ghost-free areas have, respectively, $v_0 > 0$ and $v_0 < 0$ and therefore at least one tachyon. Thus in this branch there are no ghost and tachyon-free regions. In the (T_0^-, T_L^+) branch, there is a large ghost–free region with $w_0 > 12$ (and therefore $v_0 < -1$), quite independent of the values of v_L and w_L. This ghost–free region,

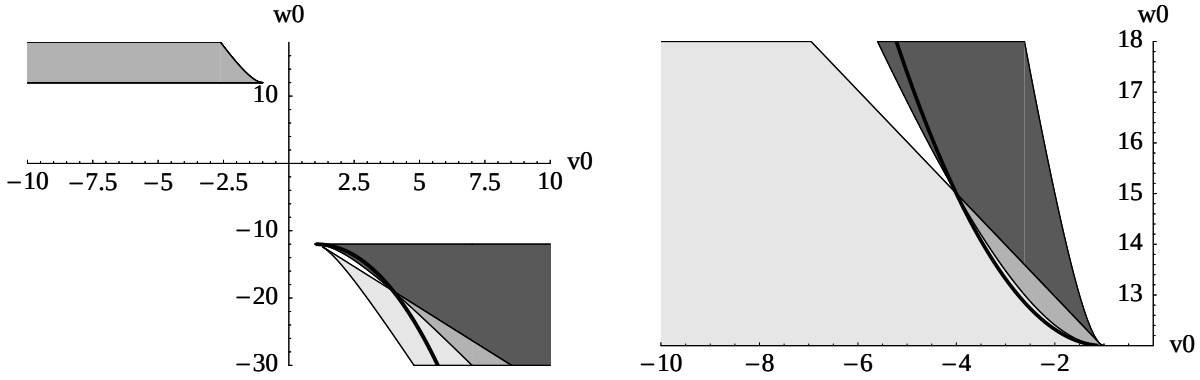

FIG. 4: Ghost-free region for both the (T_0^-, T_L^-) branch. The shades correspond to the following regions: $L > 0$ (light), $\mathcal{C}_\psi > 0$ (dark) and the intersection of both (intermediate). The region to the right of the thick black line corresponds to $\mathcal{C}_g^{(0)} > 0$. In the left panel we have $v_L = -4$, $w_L = 19$ whereas for the right panel $v_L = 4$ and $w_L = -15$.

however, always has tachyons and therefore there are no ghost and tachyon–free regions in this case, either. We do not present a figure for this case since it is quite similar to the left upper region of the left panel in Fig. 4.

In summary, in the AdS_4 case, only the (T_0^+, T_L^+) branch with $v_0 > 0$ and $v_L > 0$ has ghost and tachyon–free solutions.

B. positive curvature: dS_4 branes

We now consider the phenomenologically more relevant case of inflating branes. This corresponds to a choice of brane parameters such that $|T_i| > 1$. Recall that the absence of a true singularity in the bulk forces us to choose opposite signs for T_0 and T_L. This leaves eight different regions of parameter space: four choices of combinations $T_0^\pm$, $T_L^\pm$ times two choices of the sign of T_0. We have emphasized above the possible existence of a new source of ghosts for inflating branes, the longitudinal component of a massive graviton with mass $0 < m^2 < 2H^2$. There is a deep connection, already present in the DGP model, between the radion and the massive graviton ghosts, that can be characterized by the following identity,

$$\mathfrak{D}(q=2) = \mathrm{sign}(T_0)\,\frac{8}{3}(1+v_0T_0)(1+v_LT_L)\bar{\mathcal{C}}_\psi\,, \tag{46}$$

where we defined $\mathfrak{D}$ in (41) and $\bar{\mathcal{C}}_\psi \equiv k\mathcal{C}_\psi/\chi^2\mathcal{H}^2$ has the same sign as $\mathcal{C}_\psi$ for dS_4. This identity states that at the boundary between the regions where the radion is or is not a kinetic ghost, there is always a massive graviton with $m^2 = 2H^2$, thus also at the boundary of having a ghost longitudinal component. In the DGP model, the dependence on the brane parameters is such that, as we cross from the region where the radion is a ghost to the region where it is not, a massive graviton goes from mass squared larger than $2H^2$ to mass squared smaller than that, so that there is always a ghost in the spectrum. In our case, the richer parameter space allows for different behaviors. Let us denote by $s \equiv (v_i^*, T_i^*)$ a point for which $\bar{\mathcal{C}}_\psi(s) = \mathfrak{D}(q=2) = 0$. The variation of the solution of the equation

$$\mathfrak{D}(q) = 0, \tag{47}$$

around s for fixed v leads to (see Appendix B for details)

$$\left.\frac{\delta q}{\delta T_0}\right|_s = \frac{8}{3}\frac{1}{B(v_0,w_0,v_L,w_L)}\left.\frac{\partial\bar{\mathcal{C}}_\psi}{\partial T_0}\right|_{T_0^*}, \tag{48}$$

where $B(v_0, w_0, v_L, w_L)$ is a function that is *negative* in the region of parameter space for which $L > 0$ and *positive* otherwise. Thus, if s is in the physical region with $L > 0$, the slopes of the solution of the massive graviton and the kinetic coefficient of the radion have opposite signs, which means that *near the boundary defined by $\bar{\mathcal{C}}_\psi = 0$, either the radion or a massive graviton is always a ghost.* If, on the other hand the point s lies outside the physical region ($L < 0$) there is potentially a dramatic effect on the physical spectrum. In this case, contrary to what happens in the DGP model, there will be regions where neither the radion, nor a massive graviton is a ghost. We can study the

presence of massive gravitons with $q < 2$ in a way similar to the study of tachyons in the AdS_4 case. The behavior of $\mathfrak{D}(q)$ in the limit $q \to -\infty$ reads (see Appendix B)

$$\text{sign}[\mathfrak{D}(q \to -\infty)] = \text{sign}[T_0 v_0 v_L]. \tag{49}$$

Thus, the sign of the determinant equation at minus infinity changes when either v_0 or v_L goes through zero. Using (46) and recalling the definition of T_i we also have

$$\text{sign}[\mathfrak{D}(q=2)] = \text{sign}[T_0]\epsilon_0\epsilon_L, \quad (\text{for } \bar{\mathcal{C}}_\psi > 0), \tag{50}$$

where $\epsilon_{0,L}$ are the sign choices (branches) for $T_{0,L}^{\epsilon_{0,L}}$. A comparison of the sign of the determinant at both points shows that, excluding the graviton zero mode, there is an even (possibly zero) number of modes with $q < 2$ (*i.e.* either ghosts or tachyons) if $\text{sign}[v_0 v_L] = \epsilon_0\epsilon_L$ and an odd number of them (thus at least one) otherwise. In order to classify the different behaviors, it helps recalling that T_i^- has the opposite sign to v_i (see Fig. 1, right panel), whereas T_i^+ has the same sign as v_i everywhere except in a small wedge, where it has the opposite sign (Fig. 1, left panel).

Let us start our discussion with the cases for which the line $\bar{\mathcal{C}}_\psi = 0$ is always outside the physical region. As explained in Appendix B, this occurs in the (T_0^-, T_L^+) branch for positive T_0 and the (T_0^+, T_L^-) branch with T_0 negative or with T_0 positive and $(T_L - 1)(2 - v_L + v_L T_L)/(1 + v_L T_L) > -4$. In the latter case the radion is always a ghost whereas in the former two it is never a ghost in the physical region of parameter space. These are potentially very interesting cases, since, contrary to what happens in the DGP model, they include a self–accelerating solution with regions where neither the radion nor the longitudinal component of a massive graviton is a ghost. In this case we have $\epsilon_0\epsilon_L = -1$ and therefore the regions that satisfy $\bar{C}_\psi > 0$ with $v_0 v_L > 0$ have an odd number of modes with $q < 2$. This leaves the wedge of the brane in the (+) branch as the only possible ghost-free region. The massive graviton/radion system is actually ghost free in these regions. Unfortunately, having one of the two v_i negative makes the graviton zero mode a ghost. An example of this case is shown in Fig. 5, where we have chosen the (T_0^-, T_L^+)

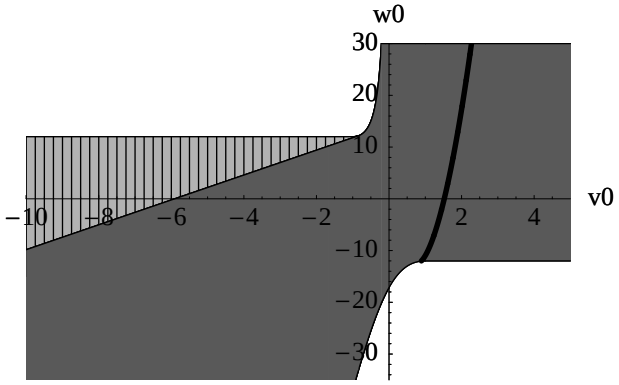

FIG. 5: Ghost and tachyon-free region for the (T_0^-, T_L^+) branch. We have chosen $v_L = 0.05$ and $w_L = -13$. The shades correspond to the following regions: $\mathcal{C}_\psi > 0$ (dark) and the intersection of $\mathcal{C}_\psi > 0$ with $L > 0$ and y_0 such that there are no singularities in the background (light). The region to the right of the thick black line corresponds to $\mathcal{C}_g^{(0)} > 0$. The hatched region corresponds to the physical region where the radion is not a ghost and there are no modes with $q < 2$. In this case the only hatched region is to the left of the thick solid line and therefore there is no ghost and tachyon free region for this branch.

branch with $v_L = 0.05$ and $w_L = -13$ (thus the brane in the (+) branch living in the small wedge). The shaded region of the figure represents the area where the radion is not a ghost, outside the physical region (dark shade) and inside the physcal region (light shade), *i.e.* $\mathcal{C}_\psi > 0$, $L > 0$ and y_0 outside the interval $[0, L]$. The curved lower boundary of the dark region represents the line $\mathcal{C}_\psi = 0$, which is outside the physical region and therefore, above it, neither the radion nor the massive graviton is a ghost. The hatched area is the physical region in which the radion is not a ghost and all massive gravitons have $q > 2$. This region is to the left of the thick solid line and therefore the graviton zero mode is a ghost.

Let us now consider the case for which the line $\bar{\mathcal{C}}_\psi = 0$ can be inside the physical region so that, *in the neighborhood* of such line, either the radion or the longitudinal component of a massive graviton is a ghost. This happens for the (T_0^-, T_L^-), (T_0^+, T_L^+) branches and for the (T_0^-, T_L^+) branch for negative T_0 or the (T_0^+, T_L^-) branch for positive T_0, provided $(T_L - 1)(2 - v_L + v_L T_L)/(1 + v_L T_L) < -4$. The condition $T_0 \cdot T_L < 0$ immediately tells us that there is an odd number of modes with $q < 2$ for the (T_0^-, T_L^-) branch, since $v_0 \cdot v_L < 0$ while $\epsilon_0\epsilon_L = +1$. Similarly, the (T_0^+, T_L^+) branch has an odd number of modes with $q < 2$ unless one (and only one) of the two branes lives in such small wedges. Numerical analysis then shows that the region with both $v_0, v_L > 0$ is ghost and tachyon–free whereas there are two

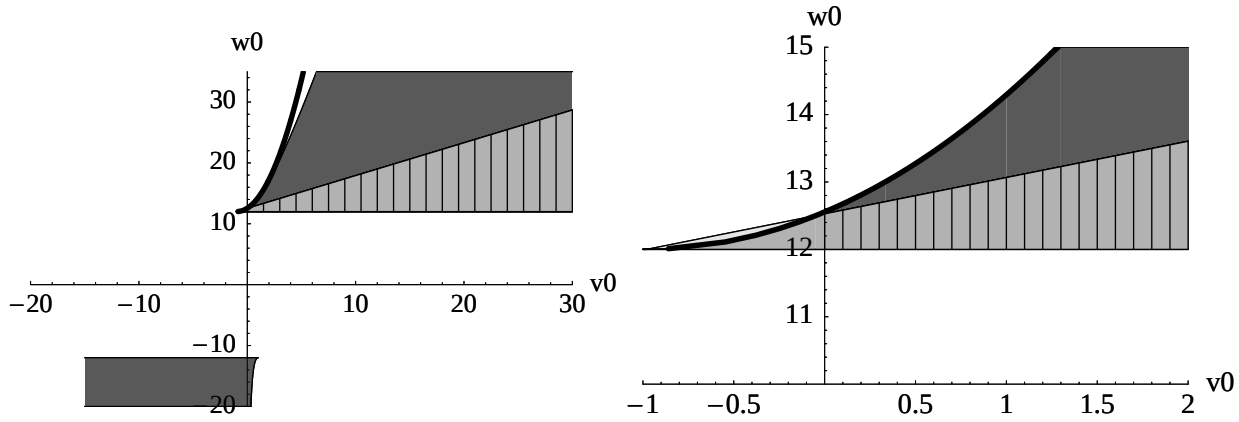

FIG. 6: Ghost and tachyon-free region for the (T_0^+, T_L^+) branch. We have chosen $v_L = 0.05$ and $w_L = -12.5$. The right panel is just a zoomed in view of the same plot. The shades correspond to the following regions: $L > 0$ and y_0 such that there are no singularities in the background (light), $\mathcal{C}_\psi > 0$ (dark) and the intersection of both (intermediate). The region to the right of the thick black line corresponds to $\mathcal{C}_g^{(0)} > 0$. The hatched region corresponds to the physical region where the radion is not a ghost and there are no modes with $q < 2$. Thus the hatched region to the right of the thick solid line is the ghost and tachyon free region.

modes with $q < 2$ if they are both negative. An example of this is shown in Fig. 6, where we have chosen $v_L = 0.05$ and $w_L = -12.5$ (thus the L brane in the small wedge). The color coding is the same as in the previous figure. This time, there is a hatched area to the right of the thick solid line (with $v_0 > 0$) that is ghost and tachyon–free. In the right panel we show a closer view of the region around $v_0 = 0$ that shows an area with intermediate shade to the right of the thick solid line for which neither the radion nor the graviton zero mode are ghosts but there is one mode with $q < 2$ (intermediate shade unhatched region with $v_0 < 0$). For the (T_0^+, T_L^-) and (T_0^-, T_L^+) branches we have $\epsilon_0 \epsilon_L = -1$, thus again only the wedge of the brane in the $(+)$ branch might give ghost free solutions. However, numerical analysis always shows two modes with $q < 2$ in the region where the radion is not a ghost.

Our discussion so far has assumed a finite L. The different properties we have described naturally generalize to an infinite extra dimension by taking the limit $L \to \infty$. Note however that, in the dS_4 case, if $y_0 > 0$, there is a different *infinte extra dimension* limit we can take, namely $L \to y_0$. This corresponds to an infinite extra dimension in conformal coordinates, for which

$$ds^2 = \hat{a}^2(x)(\gamma_{\mu\nu} dx^\mu dx^\nu + dx^2), \tag{51}$$

as shown in Appendix A. The behavior is therefore different depending on the sign of y_0. If it is negative, (*i.e.* if $T_0 < 0$), then we can take the $L \to \infty$ limit by making $T_L^\pm = 1$. This in turn is obtained for $w_L = 12$, with $v_L \geq -1$ if we are in the (T_L^+) branch and $v_L \leq -1$ in the (T_L^-) branch. Now (33) shows in this case that the graviton zero mode is non-normalizable and decouples from the spectrum whereas the radion and massive gravitons remain in the spectrum. If y_0 is positive, the limit $L \to y_0$ is obtained by taking $w_L \to -\infty$, that makes $T_L^+ \to -\infty$ or $v_L \to 0$, making $T_L^- \to -\infty$. In that case (34) shows that it is the radion which is non-normalizable while the graviton zero mode and the massive modes remain in the spectrum. Apart from the fact that either the graviton zero mode or the radion decouple, most of the features of the spectrum generalize to the infinite extra dimension case. One interesting example is the (T_0^+, T_L^-) branch with negative T_0. In that case we had regions where neither the radion nor any of the massive gravitons was a ghost or a tachyon but the graviton zero mode was always a ghost in such regions. Since $T_0 < 0$, however, we can take the $L \to \infty$ limit and the graviton zero mode decouples. Thus, this is another example that is tachyon and ghost–free. Note that this is a standard solution but contrary to the previously found ones, it has $v_L < 0$.

To sum up, we have found that only the (T_0^+, T_L^+) branch with both v_0 and v_L positive is free of ghosts and tachyons (Fig. 6, hatched area) in the case of a finite extra dimension. For an infinite extra dimension, there are also tachyon and ghost–free regions with $v_L < 0$ in the (T_0^+, T_L^-) branch. We have seen examples of self–accelerating solutions, (T_0^-, T_L^+) with T_0 positive for instance, where neither the radion nor any massive graviton is a ghost but the massless graviton is (Fig. 5, hatched area). We have seen examples of standard solutions, (T_0^+, T_L^+) for instance, where there is a ghost in the massive graviton/radion system (Fig. 6, light unhatched area). From these examples we conclude that the DGP ghost (the ghost present in the self–accelerating branch of the DGP model) is not necessarily correlated with the self–accelerating branch in our more general warped backgrounds.

V. CONCLUSIONS

The accelerating expansion of the Universe is one of the most exciting mysteries in modern science. The existence of self–accelerating solutions in braneworld gravity models suggests the possibility that an extra dimension, rather than dark energy, may explain this phenomenon. Unfortunately the original DGP model has been criticized for the presence of ghosts in the weakly-coupled regime of the self–accelerating solution. Generically either the radion or the longitudinal component of a massive graviton is a ghost.

Given the obvious importance of self–accelerating solutions, we have investigated the presence of ghosts in a generalization of the DGP model. Our model uses a warped AdS_5 bulk and two branes with arbitrary tensions and brane-localized curvature terms. Depending on functions of the input brane parameters which we have denoted as T_0, T_L, the AdS_5 bulk is sliced into sections of negative, positive, or zero curvature, giving rise to AdS_4, dS_4, or M_4 branes, respectively. For each value of the input brane parameters, there are in general two different static backgrounds per brane; the four resulting branches are denoted by $(T_0^{\pm},T_L^{\pm})$. In the dS_4 or flat case, the (T_0^-,T_L^+) and (T_0^-,T_L^-) branches provide self–accelerating solutions.

We have performed a comprehensive analysis of the spectrum for both AdS_4 and dS_4 branes and every branch, with special emphasis on the presence of ghosts. The results can be summarized as follows. For the AdS_4 brane on the (T_0^+,T_L^+) branch, the spectrum is free of ghosts and tachyons provided both localized curvature terms are positive; on all other AdS_4 branches, for all values of the input parameters, the spectrum has either ghosts or tachyons. For dS_4 branes on the (T_0^+,T_L^+) branch the spectrum is also free of ghosts and tachyons provided both localized curvature terms are positive. On all other dS_4 branches, with finite L, for all values of the input parameters, the spectrum has either ghosts or tachyons. This feature of our results is discouraging.

We find, however, solutions that depart from the general behavior of the DGP model in interesting ways. We have self–accelerating solutions which are free of DGP ghosts, *i.e.*, neither the radion nor any massive graviton are ghosts; in these cases the graviton zero mode turned out to be a ghost. In some of these solutions, one can take the second brane to infinity so that the (ghost) graviton zero mode decouples, thus obtaining another example of ghost and tachyon–free model. We also have solutions which are not self–accelerating, but nevertheless have a DGP ghost.

Although there is no self–accelerating solution that is totally ghost-free, the fact that the ghost present in the DGP model is not correlated with the self–accelerating branch makes these models an excellent laboratory to study self–acceleration. One can hope that simple modifications of these models could get rid of ghosts altogether. For example, in the case of a flat bulk it was recently suggested that adding a Gauss-Bonnet term to the bulk action will exorcise the DGP ghost [25]. Since in some cases the ghost is a radion, one could also attempt to modify the bulk scalar dynamics, in the style of Goldberger and Wise [27] (see also [28]). In this context, it is important to also consider the effects of brane matter, which requires a fully time-dependent analysis rather than the quasi-static approach taken here. Another promising direction is the study of exact solutions, using the methods developed in [29].

Acknowledgments

We are grateful for discussions with G. Dvali, R. Gregory, and N. Kaloper. MC and JL acknowledge the support of the Aspen Center for Physics, where part of this work was completed. Fermilab is operated by Universities Research Association Inc. under Contract No. DE-AC02-76CHO3000 with the U.S. Department of Energy.

APPENDIX A: COORDINATE SYSTEMS

In this Appendix we will give the $AdS_5/(A)dS_4$ background solutions in a different coordinate system that has been used in other studies of brane induced gravity models and is also the preferred one in cosmological studies. This coordinate system is conformal:

$$ds^2 = \hat{a}^2(x)(\gamma_{\mu\nu}dx^\mu dx^\nu + dx^2), \tag{A1}$$

where

$$a^2(y) = \hat{a}^2(x), \quad dy^2 = \hat{a}^2(x)dx^2. \tag{A2}$$

The coordinate change is of course different for the dS_4 and AdS_4 cases.

- **AdS_4 case**:

$$\hat{a}(x) = \frac{H}{k}\frac{1}{\sin H(x-x_0)}, \tag{A3}$$

with

$$x - x_0 = -\frac{\mathrm{i}}{2H}\ln\left(\frac{\sinh k(y-y_0)-\mathrm{i}}{\sinh k(y-y_0)+\mathrm{i}}\right), \tag{A4}$$

and

$$y = y_0 - \frac{1}{k}\sinh^{-1}\left[\cot H(x-x_0)\right]. \tag{A5}$$

Requiring that $x = 0$ for $y = 0$ we obtain

$$x_0 = -\frac{\mathrm{i}}{2H}\ln\left(\frac{\sinh ky_0-\mathrm{i}}{\sinh ky_0+\mathrm{i}}\right). \tag{A6}$$

In particular it is easy to check that

$$y - y_0 \to 0^{\pm} \;\Rightarrow\; x - x_0 \to \mp\pi/(2H), \tag{A7}$$
$$y \to \infty \;\Rightarrow\; x - x_0 \to 0^{-}. \tag{A8}$$

- **dS_4 case**:

$$\hat{a}(x) = \frac{H}{k}\frac{1}{\sinh H(x-x_0)}, \tag{A9}$$

with

$$x - x_0 = -\frac{1}{2H}\ln\left(\frac{\cosh k(y-y_0)-1}{\cosh k(y-y_0)+1}\right), \tag{A10}$$

and

$$y = y_0 - \frac{\tilde{\epsilon}_0}{k}\cosh^{-1}\left[\coth H(x-x_0)\right], \tag{A11}$$

where $\tilde{\epsilon}_0 = \text{sign } T_0$. Again, requiring that $x = 0$ for $y = 0$ we obtain

$$x_0 = \frac{1}{2H}\ln\left(\frac{\cosh ky_0-1}{\cosh ky_0+1}\right). \tag{A12}$$

In this case we have

$$y \to y_0 \;\Rightarrow\; x \to \infty, \tag{A13}$$
$$y \to \infty \;\Rightarrow\; x - x_0 \to 0. \tag{A14}$$

APPENDIX B: DETAILED CALCULATIONS FOR dS_4 BRANES

We reproduce in this appendix the detailed calculations that lead to the determination of ghosts and tachyons for dS_4 branes. For convenience, we will use (v, T) as independent variables. The first step is to characterize the region of parameter space satisfying $\bar{C}_\psi = 0$. Let us fix the value of (v_L, T_L), and solve $\bar{\mathcal{C}}_\psi(v_0^*, T_0^*) = 0$ for v_0^*:

$$v_0^* = \frac{-2T_0^* - 2 - \chi_L}{(T_0^*+1)^2 + \chi_L T_0^*}, \tag{B1}$$

where

$$\chi_L = \frac{(T_L-1)(2 - v_L + v_L T_L)}{1 + v_L T_L}. \tag{B2}$$

In the (v_0, T_0)–plane, the allowed regions are bounded by $T_0 = \pm 1$ or $T_0 = -T_L$, and $T_0 = -1/v_0$. For example, the allowed region for the (T_0^-, T_L^-) branch with $T_0^- < 0$ lies in the fourth quadrant with $T_0 < -T_L$ and $T_0 < -1/v_0$. In this case, in order for the $\bar{C}_\psi = 0$ line to fit in the allowed region, it should be satisfied that v_0^* of (B1) be larger than $-1/T_0^*$. This inequality can change sign for some of the branches.

Therefore, to see whether $\bar{C}_\psi = 0$ line lies inside or outside of the allowed region, we need to check the sign of

$$v_0^* + \frac{1}{T_0^*} = \frac{1 - T_0^{*2}}{T_0^*} \frac{1}{T_0^{*2} + (2 + \chi_L) T_0^* + 1}\,, \tag{B3}$$

whose only nontrivial part is

$$\mathfrak{S}(T_0) = T_0^{*2} + (2 + \chi_L) T_0^* + 1\,. \tag{B4}$$

Since $T_0 < -T_L < -1$ or $1 < T_0 < -T_L$, from the elementary analysis on quadratic functions it would suffice to determine the signs of

$$\mathfrak{S}(-T_L) = \frac{1 - T_L^2}{1 + v_L T_L}\,, \quad \mathfrak{S}(1) = 4 + \chi_L\,, \tag{B5}$$

and the location of the symmetry axis, $l = -(2 + \chi_L)/2$, relative to $-T_L$ or 1. Note that the sign of $\mathfrak{S}(-T_L)$ is the opposite of ϵ_L. The result is summarized in the following table:

		$\mathfrak{S}(-T_L)$	$\mathfrak{S}(1)$	l	sign[(B3)]	allowed region	location of $C_\psi = 0$
$T_0 < 0$	(T_0^+, T_L^+)	$-$			$+ \to -$ as T_0 increases	$v_0 + 1/T_0 < 0$	inside or outside
	(T_0^+, T_L^-)	$+$		$> -T_L$	$+$	$v_0 + 1/T_0 < 0$	outside
	(T_0^-, T_L^+)	$-$			$+ \to -$ as T_0 increases	$v_0 + 1/T_0 > 0$	inside or outside
	(T_0^-, T_L^-)	$+$		$> -T_L$	$+$	$v_0 + 1/T_0 > 0$	inside
$T_0 > 0$	(T_0^+, T_L^+)	$-$	$-$		$+$	$v_0 + 1/T_0 > 0$	inside
	(T_0^+, T_L^-)	$+$	$+$	< 1	$-$	$v_0 + 1/T_0 > 0$	outside
			or $-$		$+ \to -$ as T_0 increases	$v_0 + 1/T_0 > 0$	inside or outside
	(T_0^-, T_L^+)	$-$	$-$		$+$	$v_0 + 1/T_0 < 0$	outside
	(T_0^-, T_L^-)	$+$	$+$	< 1	$-$	$v_0 + 1/T_0 < 0$	inside
			or $-$		$+ \to -$ as T_0 increases	$v_0 + 1/T_0 < 0$	inside or outside

A blank in the tables denotes that the corresponding information does not affect the result. $+ \to -$ as T_0 increases means that both signs are possible, depending on the parameters. Comparing the sign of (B3) with the allowed region for each case (columns 4 and 5 in the table) we obtain the classification of the last column in the table.

Let us assume the line of $\bar{C}_\psi = 0$ is inside the allowed region, with (v_0^*, T_0^*) representing the locus. The treatment of the solution is different depending on the sign of T_0. If T_0 is negative, so that z is positive, we get, from (30,34),

$$\begin{aligned} \mathfrak{D}(q = 2) &= 4(T_0 + 1)(2 + v_0 + v_0 T_0)(1 + v_L T_L) + 4(T_L - 1)(2 - v_L + v_L T_L)(1 + v_0 T_0) \\ &= -\frac{8}{3}(1 + v_0 T_0)(1 + v_L T_L)\bar{\mathcal{C}}_\psi\,, \end{aligned} \tag{B6}$$

and therefore if $\bar{\mathcal{C}}_\psi = 0$ has a solution, there is a KK graviton mode with $q = 2$. Let us now consider how $\bar{\mathcal{C}}_\psi$ and $\mathfrak{D}$ change as we vary T_0 around the solution: for given L-parameters, when $s = (q = 2, T_0 = T_0^*)$ solves $\mathfrak{D} = 0$, at $(q = 2 + \delta q, T_0 = T_0^* + \delta T_0)$ which is another solution in a small neighborhood of s, we have

$$\begin{aligned} 0 &= \mathfrak{D}(T_0^* + \delta T_0, 2 + \delta q) = \mathfrak{D}(s) + \frac{\partial \mathfrak{D}}{\partial T_0}\Big|_s \delta T_0 + \frac{\partial \mathfrak{D}}{\partial q}\Big|_s \delta q \\ &= 0 - \frac{8}{3}(1 + v_0 T_0)(1 + v_L T_L)\, \frac{\partial \bar{\mathcal{C}}_\psi}{\partial T_0}\Big|_{T_0^*} \delta T_0 + \frac{\partial \mathfrak{D}}{\partial q}\Big|_s \delta q\,, \end{aligned} \tag{B7}$$

i.e.,

$$\frac{\delta q}{\delta T_0} = \frac{8}{3} \frac{(1 + v_0 T_0)(1 + v_L T_L)}{\partial \mathfrak{D}/\partial q|_s}\, \frac{\partial \bar{\mathcal{C}}_\psi}{\partial T_0}\Big|_{T_0^*}\,. \tag{B8}$$

To evaluate $\partial\mathfrak{D}/\partial q$, we use [31] 3.7 (6), [30] 4.224.9 and [31] 3.6.1 (8) to get

$$\partial_\nu P_\nu^0(z)|_{\nu=0} = \ln\frac{z+1}{2}\,, \tag{B9}$$

$$\partial_\nu P_\nu^{-1}(z)|_{\nu=0} = -\sqrt{\frac{z-1}{z+1}}+\sqrt{\frac{z+1}{z-1}}\ln\frac{z+1}{2}\,, \tag{B10}$$

$$\partial_\nu P_\nu^{-2}(z)|_{\nu=0} = -\frac{3z+1}{4(z+1)}+\frac{z+1}{2(z-1)}\ln\frac{z+1}{2}\,. \tag{B11}$$

Also using [30] 8.712, 2.727.2 and [31] 3.6.1 (5) we obtain

$$\begin{aligned}\partial_\nu Q_\nu^0(z)|_{\nu=0} &= \frac{1}{2}\ln 2\ln\frac{z+1}{z-1}+\frac{1}{4}\ln(z^2-1)\ln\frac{z-1}{z+1}\\ &\quad -\frac{1}{2}\mathrm{Li}_2\Big(\frac{2}{1+z}\Big)+\frac{1}{2}\mathrm{Li}_2\Big(\frac{2}{1-z}\Big)\,,\end{aligned} \tag{B12}$$

$$\partial_\nu Q_\nu^1(z)|_{\nu=0} = \frac{1}{2\sqrt{z^2-1}}\Big(z\ln\frac{z+1}{z-1}+\ln\frac{z^2-1}{4}\Big)\,, \tag{B13}$$

$$\partial_\nu Q_\nu^2(z)|_{\nu=0} = -\frac{1}{2(z^2-1)}\Big\{(z^2+1)\ln\frac{z+1}{z-1}+2z\ln\frac{z^2-1}{4}\Big\}\,, \tag{B14}$$

where $\mathrm{Li}_2(z)$ is the dilogarithm function, defined as

$$\mathrm{Li}_2(z)=\sum_{k=1}^{\infty}\frac{z^k}{k^2}=\int_z^0\frac{\ln(1-t)}{t}\mathrm{d}t\,. \tag{B15}$$

Then, $\partial\mathfrak{D}/\partial q|_{q=2}$ becomes

$$\begin{aligned}\frac{\partial\mathfrak{D}}{\partial q}\Big|_{q=2} &= 4(1+v_LT_L)\Big\{2(T_0+1)(1+v_0T_0)+(2-v_0+v_0T_0)(-T_0+1)\ln\frac{-T_0+1}{2}\Big\}\\ &\quad +(2-v_L+v_LT_L)(T_L-1)\Big\{(v_0+2T_0+v_0T_0^2)\ln\frac{-T_0-1}{-T_0+1}+2(1+v_0T_0)\Big(1+\ln\frac{T_0^2-1}{4}\Big)\Big\}\\ &\quad +4(1+v_0T_0)\Big\{2(T_L-1)(1+v_LT_L)-(2+v_L+v_LT_L)(T_L+1)\ln\frac{T_L+1}{2}\Big\}\\ &\quad -(2+v_0+v_0T_0)(T_0+1)\Big\{(v_L+2T_L+v_LT_L^2)\ln\frac{T_L-1}{T_L+1}-2(1+v_LT_L)\Big(1+\ln\frac{T_L^2-1}{4}\Big)\Big\}\,.\end{aligned} \tag{B16}$$

At $T_0=T_0^*$, (B6)$=0$ simplifies the above into

$$\frac{\partial\mathfrak{D}}{\partial q}\Big|_s = \frac{(T_0^{*2}-1)(T_L^2-1)}{(T_L-1)^2-\chi_LT_L}\cdot\frac{8(T_0^*+T_L)-\chi_L^2\ln\frac{-T_0^*-1}{T_L-1}+(\chi_L+4)^2\ln\frac{-T_0^*+1}{T_L+1}}{(T_0^*+1)^2+\chi_LT_0^*}\,, \tag{B17}$$

and (B8) becomes

$$\frac{\delta q}{\delta T_0}\Big|_s=\frac{8}{3B(T_0;T_L,\chi_L)}\frac{\partial\bar{\mathcal{C}}_\psi}{\partial T_0}\Big|_{T_0^*}\,, \tag{B18}$$

where

$$B=8(T_0^*+T_L)-\chi_L^2\ln\frac{-T_0^*-1}{T_L-1}+(\chi_L+4)^2\ln\frac{-T_0^*+1}{T_L+1}\,. \tag{B19}$$

B is a growing function of T_0,

$$\frac{\mathrm{d}B}{\mathrm{d}T_0}=2\frac{(2+2T_0+\chi_L)^2}{T_0^2-1}>0\,. \tag{B20}$$

For $L>0$ we have $T_0<-T_L$ and therefore B is bounded above by $B(-T_L)=0$, or in other words, it is always negative. If $L<0$, on the other hand, we have $T_0>-T_L$ and therefore B is bounded below by 0, so it is positive.

Thus, when $\bar{\mathcal{C}}_\psi = 0$ has a solution in the physical region (with $L > 0$), the slope of the mass of the first KK graviton mode when it passes $q = 2$ and that of $\bar{\mathcal{C}}_\psi$ when it crosses zero have opposite signs, and therefore when the first KK graviton mode is heavier than $2H^2$ the radion is a ghost and *vice versa*. If $\bar{\mathcal{C}}_\psi = 0$ has a solution outside the physical region (where $L < 0$), then both the radion and the longitudinal component of a massive graviton are ghosts at one side of the line (in the (v_0, w_0) plane) and neither of them is at the other side.

If T_0 is positive, then z is negative in the physical region and we have to use the wave functions evaluated at $-z$ for the massive gravitons. This introduces some extra minus signs, so that now we have

$$\mathfrak{D}(q=2) = \frac{8}{3}(1+v_0T_0)(1+v_LT_L)\bar{\mathcal{C}}_\psi\,, \tag{B21}$$

$$\frac{\delta q}{\delta T_0}\Big|_s = -\frac{8}{3}\frac{(1+v_0T_0)(1+v_LT_L)}{\partial\mathfrak{D}/\partial q|_s}\,\frac{\partial\bar{\mathcal{C}}_\psi}{\partial T_0}\Big|_{T_0^*}\,, \tag{B22}$$

$$\frac{\partial\mathfrak{D}}{\partial q}\Big|_s = -\frac{(T_0^{*2}-1)(T_L^2-1)}{(T_L-1)^2-\chi_L T_L}\cdot\frac{8(T_0^*+T_L)-\chi_L^2\ln\frac{T_0^*+1}{-T_L+1}+(\chi_L+4)^2\ln\frac{T_0^*-1}{-T_L-1}}{(T_0^*+1)^2+\chi_L T_0^*}\,. \tag{B23}$$

These extra minuses get cancelled among themselves, and we still get the same final result, (B18-B19). Thus independently of the sign of T_0, it is always true that, near the locus of points satisfying $\bar{\mathcal{C}}_\psi = 0$, either the radion or the longitudinal component of a massive graviton with $m^2 < 2H^2$ is a ghost if parameters are chosen from inside the physical region and neither of them is to one side of the region $\bar{\mathcal{C}}_\psi = 0$ if that region has $L < 0$.

Let us now compute the limit $\mathfrak{D}(q \to -\infty)$, which is equivalent to $\nu \to \infty$, where ν is the index of the corresponding Legendre function. The calculation is again different for the two signs of T_0. We start considering the case of negative T_0, so that z is positive. Using 8.723 1 from [30] we find

$$P^{-2}_{\nu\to\infty}(\cosh\alpha) \sim \frac{1}{\sqrt{\pi}}\frac{e^{(\nu+1)\alpha}}{\sqrt{e^{2\alpha}-1}}\nu^{-5/2}, \tag{B24}$$

where we have defined $z \equiv \cosh\alpha$. Then

$$(1-z^2)\frac{d}{dz}P^{-2}_{\nu\to\infty}(\cosh\alpha) \sim -\frac{1}{2\sqrt{\pi}}\sqrt{e^{2\alpha}-1}e^{\nu\alpha}\nu^{-3/2}. \tag{B25}$$

Using now 8.723 2 and 8.732 1 from [30], respectively, we get

$$Q^2_{\nu\to\infty}(\cosh\alpha) \sim \sqrt{\pi}\frac{e^{-\nu\alpha}}{\sqrt{e^{2\alpha}-1}}\nu^{3/2}, \tag{B26}$$

$$(1-z^2)\frac{d}{dz}Q^2_{\nu\to\infty}(\cosh\alpha) \sim \frac{\sqrt{\pi}}{2}\sqrt{e^{2\alpha}-1}e^{-(\nu+1)\alpha}\nu^{5/2}. \tag{B27}$$

These expressions allow us to compute the limit of the different coefficients, that turns out to be identical for both branes

$$a_i(q\to-\infty) \sim \frac{v_i(T_i^2-1)}{\sqrt{\pi}}\frac{e^{(\nu-1)\alpha_i}}{\sqrt{e^{2\alpha_i}-1}}\nu^{-1/2}, \tag{B28}$$

$$b_i(q\to-\infty) \sim \sqrt{\pi}v_i(T_i^2-1)\frac{e^{-\nu\alpha_i}}{\sqrt{e^{2\alpha_i}-1}}\nu^{7/2}. \tag{B29}$$

We can now compute the limit of the full determinant,

$$\begin{aligned} a_0b_L - a_Lb_0 &\sim v_0v_L\frac{T_0^2-1}{\sqrt{e^{2\alpha_0}-1}}\frac{T_L^2-1}{\sqrt{e^{2\alpha_L}-1}}\nu^3\Big[e^{-\alpha_0}e^{\nu(\alpha_0-\alpha_L)}-e^{-\alpha_L}e^{\nu(\alpha_L-\alpha_0)}\Big] \\ &\sim v_0v_L\frac{T_0^2-1}{\sqrt{e^{2\alpha_0}-1}}\frac{T_L^2-1}{\sqrt{e^{2\alpha_L}-1}}\nu^3e^{-\alpha_0}e^{\nu(\alpha_0-\alpha_L)}, \end{aligned} \tag{B30}$$

where we have used that, in the physical region with negative T_0, we have $0 < T_L < -T_0 \Rightarrow \cosh\alpha_L < \cosh\alpha_0 \Rightarrow \alpha_L < \alpha_0$. Thus,

$$\mathrm{sign}\big[\mathfrak{D}(q\to-\infty)\big] = -\mathrm{sign}\big[v_0v_L\big] = \mathrm{sign}\big[T_0v_0v_L\big]. \tag{B31}$$

We can now check what happens in the case that $T_0 > 0$ so that $z < 0$. As we said above, the valid solution is then the corresponding associated Legendre functions evaluated at $-z$. The expression of the a_i and b_i is then identical to (30) with the change $\theta_i \to -\theta_i$, *i.e.*

$$c_0^{(T_0>0)}(T_0) = c_L^{(T_0<0)}(T_0), \quad c_L^{(T_0>0)}(T_L) = c_0^{(T_0<0)}(T_L), \tag{B32}$$

where c_i stands for any of a_i or b_i. Thus, noting that now $0 < T_0 < -T_L \Rightarrow \cosh\alpha_0 < \cosh\alpha_L \Rightarrow \alpha_0 < \alpha_L$ in the physical region, we get

$$\begin{aligned} a_0 b_L - a_L b_0\Big|_{T_0>0} &\sim v_0 v_L \frac{T_0^2-1}{\sqrt{e^{2\alpha_0}-1}} \frac{T_L^2-1}{\sqrt{e^{2\alpha_L}-1}} \nu^3 \Big[e^{-\alpha_0} e^{\nu(\alpha_0-\alpha_L)} - e^{-\alpha_L} e^{\nu(\alpha_L-\alpha_0)}\Big] \\ &\sim -v_0 v_L \frac{T_0^2-1}{\sqrt{e^{2\alpha_0}-1}} \frac{T_L^2-1}{\sqrt{e^{2\alpha_L}-1}} \nu^3 e^{-\alpha_L} e^{\nu(\alpha_L-\alpha_0)}, \end{aligned} \tag{B33}$$

and therefore

$$\mathrm{sign}\big[\mathfrak{D}^{(T_0>0)}(q\to-\infty)\big] = \mathrm{sign}\big[v_0 v_L\big] = \mathrm{sign}\big[T_0 v_0 v_L\big]. \tag{B34}$$

APPENDIX C: FLAT BULK LIMIT

In this appendix we will show how to obtain the limit of a flat bulk ($k \to 0$) for dS_4 branes. Taking the $k \to 0$ limit in the $\mathrm{AdS}_5/\mathrm{dS}_4$ background needs special care because our usual reparametrization of the extra dimensional coordinate y, $z = \coth k(y-y_0)$, breaks down and the input parameters, $v_i = kM_i^2/M^3$ and $w_i = V_i/2kM^3$, are ill-defined. Therefore, it is easier to redo our analysis directly with $k = 0$. That is, we work on an $\mathrm{M}_5/\mathrm{dS}_4$ background. Let us define the following combinations of brane parameters and the fundamental Planck mass,

$$\lambda_i \equiv \frac{M_i^2}{M^3}, \quad U_i \equiv \frac{V_i}{2M^3}. \tag{C1}$$

Solving for the background is straightforward, and we get

$$G^{(0)}_{MN}\mathrm{d}x^M\mathrm{d}x^N = a^2(y)\gamma_{\mu\nu}\mathrm{d}x^\mu\mathrm{d}x^\nu + \mathrm{d}y^2\,, \tag{C2}$$

where $a = 1 + \epsilon_0\mathcal{H}y$ with $\epsilon_0 = +1$ for the self–accelerating branch and $\epsilon_0 = -1$ for the standard one. Here $\gamma_{\mu\nu}$ is the dS_4 metric. The values of $\mathcal{H}$ and L are determined by the brane-boundary equations:

$$0 = \frac{\lambda_0}{2}\mathcal{H}^2 - \epsilon_0\mathcal{H} - \frac{U_0}{12}\,, \tag{C3}$$

$$0 = \frac{\lambda_L}{2}\Big(L + \frac{\epsilon_0}{\mathcal{H}}\Big)^{-2} + \Big(L + \frac{\epsilon_0}{\mathcal{H}}\Big)^{-1} - \frac{U_L}{12}\,. \tag{C4}$$

We first look at the radion. Following footsteps of §5 of [8], we can get the equations of motion for the massless scalar degrees of freedom. Solving them, we obtain

$$\varphi_1(x,y) = -\frac{f_2(x)}{\mathcal{H}^2} + \frac{C(x)}{a^{(3-\epsilon_0)/2}} + \frac{D(x)}{a^{(3+\epsilon_0)/2}} - \mathfrak{F}(y)\psi(x)\,, \tag{C5}$$

$$\varphi_2(x,y) = f_2(x) + \Big(\frac{a'}{a}\mathcal{F}(y) + \mathcal{H}^2\mathfrak{F}(y)\Big)\psi(x)\,. \tag{C6}$$

$f_2(x)$ turns out to be a pure gauge field and will be killed. Plugging (C5) into the brane-boundary equations gives

$$\alpha_i C + \beta_i D = \frac{\mathcal{F}(y_i)}{\mathcal{H}}\psi\,, \tag{C7}$$

where

$$\alpha_i = -\frac{\theta_i(3\epsilon_0-1)/2\cdot a_i^{-(1-\epsilon_0)/2} + \lambda_i\mathcal{H}a_i^{-(3-\epsilon_0)/2}}{\theta_i + \epsilon_0\lambda_i\mathcal{H}/a_i}\,, \tag{C8}$$

$$\beta_i = -\frac{\theta_i(3\epsilon_0+1)/2\cdot a_i^{-(1+\epsilon_0)/2} + \lambda_i\mathcal{H}a_i^{-(3+\epsilon_0)/2}}{\theta_i + \epsilon_0\lambda_i\mathcal{H}/a_i}\,, \tag{C9}$$

with $a_i = a(y_i)$.

At the massive level, a solution of the bulk equations of motion is now

$$b_{\mu\nu}(x,y) = a^{(1-\sqrt{9-4q})/2} A_{\mu\nu}(x) + a^{(1+\sqrt{9-4q})/2} B_{\mu\nu}(x)\,, \tag{C10}$$

and the brane-boundary equations provide the determinant equation, which gives the mass spectrum;

$$\begin{aligned} 0 \;&=\; \{(3+\sqrt{9-4q})\epsilon_0 - \mathcal{H}\lambda_0 q\}\cdot a_L^{(-3+\sqrt{9-4q})/2}\{(-3+\sqrt{9-4q})(\epsilon_0+\mathcal{H}L) - \mathcal{H}\lambda_L q\} \\ &-\; \{(-3+\sqrt{9-4q})\epsilon_0 + \mathcal{H}\lambda_0 q\}\cdot a_L^{-(3+\sqrt{9-4q})/2}\{(3+\sqrt{9-4q})(\epsilon_0+\mathcal{H}L) + \mathcal{H}\lambda_L q\}\,. \end{aligned} \tag{C11}$$

Let's look into the self–accelerating branch($\epsilon_0 = +1$). Here, since $\alpha_0 = \alpha_L = -1$, we can fix the gauge function $F(y)$ such that $\mathcal{F}(y_i) = \chi\beta_i$ with the constant χ a residual gauge parameter. This choice kills the C mode and

$$D = \frac{\chi}{\mathcal{H}}\psi\,, \tag{C12}$$

which redefines (26) for $\mathrm{M}_5/\mathrm{dS}_4$ background;

$$\mathcal{Y}_1(y) = \frac{\chi}{\mathcal{H}}a^{-2} - \mathfrak{F}\,,\;\; \mathcal{Y}_2(y) = \chi\mathcal{H}a^{-2} + \frac{\mathcal{H}}{a}\mathcal{F}\,. \tag{C13}$$

Working out the quadratic action, we finally get

$$C_\psi = \frac{3\chi^2 H}{2}\sum_i \Big(\frac{y_i}{y_i+1/H} - \frac{1}{\theta_i + H(y_i+\lambda_i)}\Big)\,. \tag{C14}$$

Also with $\epsilon_0 = +1$, (C11) becomes

$$\begin{aligned} 0 \;&=\; \{(3+\sqrt{9-4q}) - \mathcal{H}\lambda_0 q\}\cdot a_L^{(-3+\sqrt{9-4q})/2}\{(-3+\sqrt{9-4q})(1+\mathcal{H}L) - \mathcal{H}\lambda_L q\} \\ &-\; \{(-3+\sqrt{9-4q}) + \mathcal{H}\lambda_0 q\}\cdot a_L^{-(3+\sqrt{9-4q})/2}\{(3+\sqrt{9-4q})(1+\mathcal{H}L) + \mathcal{H}\lambda_L q\}\,. \end{aligned} \tag{C15}$$

We can match the above with the recent results of Izumi *et al.* for braneworld models on a $\mathrm{M}_5/\mathrm{dS}_4$ background with a finite extra dimension [28]. The conversion from our setup to theirs can be achieved by the following identifications: $\lambda_0, \lambda_L \to 2r_c$, $V_i \to \tau_i$. Then correspondence among derived quantities follows: $\mathcal{H} \to H_+ = \hat{H}_+ + 1/r_c$, $L \to 1/H_- - 1/H_+$, $q \to m_i^2$. Upon making these substitutions, (C14) and (C15) turn into

$$\begin{aligned} C_\psi \;&=\; 3\chi^2(\hat{H}_+ - H_-)\frac{1+(1+2\hat{H}_+ r_c)(1+2H_- r_c)}{(1+2\hat{H}_+ r_c)(1+2H_- r_c)} \\ &=\; 3\chi^2\Big\{\frac{\hat{H}_+(1+\hat{H}_+ r_c)}{1+2\hat{H}_+ r_c} - \frac{H_-(1+H_- r_c)}{1+2H_- r_c}\Big\}\,. \end{aligned} \tag{C16}$$

This expression is a positive constant times times the expression in eqn. (2.42) of [28]. Similarly:

$$\begin{aligned} 0 \;&=\; \Big(3 - 2H_+ r_c m_i^2 + \sqrt{9-4m_i^2}\Big) \\ &\quad\times\Big(\frac{H_+}{H_-}\Big)^{(-1+\sqrt{9-4m_i^2})/2}\Big(-3 - 2H_- r_c m_i^2 + \sqrt{9-4m_i^2}\Big) \\ &\quad-\Big(3 - 2H_+ r_c m_i^2 - \sqrt{9-4m_i^2}\Big) \\ &\quad\times\Big(\frac{H_+}{H_-}\Big)^{-(1+\sqrt{9-4m_i^2})/2}\Big(-3 - 2H_- r_c m_i^2 - \sqrt{9-4m_i^2}\Big)\,, \end{aligned} \tag{C17}$$

which is $4H_-$ times the determinant of the expression in eqn. (2.35) of [28]. The normal branch solutions ($\epsilon_0 = -1$) can be worked out similarly.

---

[1] C. Deffayet, Phys. Lett. B **502**, 199 (2001) [arXiv:hep-th/0010186].

[2] C. Deffayet, G. R. Dvali and G. Gabadadze, Phys. Rev. D **65**, 044023 (2002) [arXiv:astro-ph/0105068].
[3] G. R. Dvali, G. Gabadadze and M. Porrati, Phys. Lett. B **485**, 208 (2000) [arXiv:hep-th/0005016].
[4] K. Koyama, Phys. Rev. D **72**, 123511 (2005) [arXiv:hep-th/0503191]; D. Gorbunov, K. Koyama and S. Sibiryakov, Phys. Rev. D **73**, 044016 (2006) [arXiv:hep-th/0512097]; C. Charmousis, R. Gregory, N. Kaloper and A. Padilla, arXiv:hep-th/0604086.
[5] M. A. Luty, M. Porrati and R. Rattazzi, JHEP **0309**, 029 (2003) [arXiv:hep-th/0303116].
[6] A. Nicolis and R. Rattazzi, JHEP **0406**, 059 (2004) [arXiv:hep-th/0404159].
[7] A. Karch and L. Randall, JHEP **0105**, 008 (2001) [arXiv:hep-th/0011156].
[8] M. Carena, J. D. Lykken and M. Park, Phys. Rev. D **72**, 084017 (2005) [arXiv:hep-ph/0506305].
[9] R. Bao, M. Carena, J. Lykken, M. Park and J. Santiago, Phys. Rev. D **73**, 064026 (2006) [arXiv:hep-th/0511266].
[10] J. M. Cline, S. Jeon and G. D. Moore, Phys. Rev. D **70**, 043543 (2004) [arXiv:hep-ph/0311312].
[11] N. Arkani-Hamed, H. C. Cheng, M. A. Luty and S. Mukohyama, JHEP **0405**, 074 (2004) [arXiv:hep-th/0312099].
[12] A. Adams, N. Arkani-Hamed, S. Dubovsky, A. Nicolis and R. Rattazzi, arXiv:hep-th/0602178.
[13] A. Jenkins and D. O'Connell, arXiv:hep-th/0609159.
[14] A. Higuchi, Nucl. Phys. B **282**, 397 (1987).
[15] A. Higuchi, J. Math. Phys. **28**, 1553 (1987) [Erratum-ibid. **43**, 6385 (2002)].
[16] T. Garidi, J. P. Gazeau and M. V. Takook, J. Math. Phys. **44**, 3838 (2003) [arXiv:hep-th/0302022].
[17] S. Deser and A. Waldron, Phys. Lett. B **508**, 347 (2001) [arXiv:hep-th/0103255].
[18] S. Deser and R. I. Nepomechie, Annals Phys. **154**, 396 (1984).
[19] S. Deser and A. Waldron, Phys. Rev. Lett. **87**, 031601 (2001) [arXiv:hep-th/0102166].
[20] C. Deffayet, G. Gabadadze and A. Iglesias, JCAP **0608**, 012 (2006) [arXiv:hep-th/0607099].
[21] S. Weinberg, *Gravitation and Cosmology*, John Wiley & son, New York, 1972.
[22] G. Gabadadze and A. Iglesias, Phys. Lett. B **632**, 617 (2006) [arXiv:hep-th/0508201].
[23] A. Gruzinov, M. Kleban, M. Porrati and M. Redi, arXiv:astro-ph/0609553.
[24] E. W. Kolb, S. Matarrese and A. Riotto, arXiv:astro-ph/0506534.
[25] C. de Rham and A. J. Tolley, JCAP **0607**, 004 (2006) [arXiv:hep-th/0605122].
[26] L. Randall and R. Sundrum, Phys. Rev. Lett. **83**, 3370 (1999) [arXiv:hep-ph/9905221]; Phys. Rev. Lett. **83**, 4690 (1999) [arXiv:hep-th/9906064].
[27] W. D. Goldberger and M. B. Wise, Phys. Rev. Lett. **83**, 4922 (1999) [arXiv:hep-ph/9907447].
[28] K. Izumi, K. Koyama and T. Tanaka, arXiv:hep-th/0610282.
[29] N. Kaloper, Phys. Rev. Lett. **94**, 181601 (2005) [Erratum-ibid. **95**, 059901 (2005)] [arXiv:hep-th/0501028]; Phys. Rev. D **71**, 086003 (2005) [Erratum-ibid. D **71**, 129905 (2005)] [arXiv:hep-th/0502035].
[30] I. S. Gradshtein and I. M. Ryzhik, *Table of Integrals, Series and Products*, Academic Press, New York, 1980.
[31] *Bateman Manuscript Project: Higher Transcendental Functions*, Volume I; ed. A Erdelyi, McGraw-Hill, New York, 1953.